Preparation and Characterization of Fe-containing Mesoporous HZSM-5 Catalysts for Automotive Exhaust Cleaning

Yi Liang[1,a], Yongwan Gu[2,b], Changfu Zhuang[1,c], Zhengjun Shi[1,d],Ying Wang[1,e], Chunhua Wu[1,f*]

(1 College of Chemical Engineering, Southwest Forestry University, 650224,Kunming, Yunnan Province, PRC;

2 Kunming Sino-Platinum Metals Catalyst Co. Ltd., 650106, Kunming,Yunnan Province, PRC)

([a]1428129092@qq.com, [b]guyongwan@163.com, [c]81130477@qq.com，[d]502337798@qq.com，[e]254660352@qq.com，[f*]906072220@qq.com)

* Corresponding author: Tel.: +86 15925150719, E-mail address: 906072220@qq.com.

Keywords: Mesoporous ZSM-5; Fe/ZSM-5; Auto-exhaust catalyst; Preparation; Characterization; Catalytic activity

Abstract: Mesoporous HZSM-5was prepared by alkali solution treating microporous HZSM-5, then Fe/ZSM-5 catalysts have been successfully fabricated by equal volume impregnation method. Their texture structure, crystal phase structure and acidity were characterized by N_2 physisorption /desorption, XRD, SEM and NH_3-TPD techniques. The results show that mesoporous surface area and mesoporous pore volume of the ZSM-5 after alkali treatment increased obviously from 77m^2/g and 0.086cm^3/g to 192m^2/g and 0.326cm^3/g respectively. XRD patterns show the crystallinity of the zeolite treated by alkali decreased gradually with the increase of alkali concentration. The XRD patterns of the $FeCl_3$/ZSM-5 samples show that the high $FeCl_3$ dispersion in the zeolites treated by alkali. All zeolites have the MFI framework topology. When Fe-ZSM-5 is used as catalyst for cleaning auto-exhaust, the catalytic effect of mesoporous molecular sieve loaded with $FeCl_3$ is more active than HZSM-5.

Introduction

In the past decades, environmental protection has become an increasing worldwide concern. Automobile exhaust is a major cause of air pollution[1,2]. Vehicle exhaust is complex and contains hundreds of different compounds, monoxide (CO), hydrocarbon (HC) and nitric oxide (NO_X) are the main causes of air pollution[3-5].Three-way catalysts (TWCs) are one of the most important technologies for automotive emission control[6,7]. TWCs can work simultaneously and efficiently to reduce NO and to oxidize CO and hydrocarbons at the theoretical air/fuel (A/F) ratio of around 14.6. Basically, TWCs are composed of precious metals (Pt, Pd and Rh) as the catalytically active components[8-10], support such as Al_2O_3 and cerium oxide based material as an oxygen storage component to widen the operational A/F window[11-14]. Although the technologies of TWCs are well-established, further improvement of catalytic efficiency and stability is still required because automotive emission regulations are becoming more and more stringent in the world.

Selective catalytic reduction (SCR) with ammonia-containing precursors, such as urea, is an efficient method to eliminate NOx emissions from the exhaust of diesel vehicles and stationary

combustion processes [15-19]. Many metal-exchanged zeolites (ZSM-5, MOR, BEA and FER) have been shown to be active catalysts for the NH_3-SCR of NO [20-23]. Molecular sieve and modified molecular sieve materials are considered as selective catalytic reduction catalysts because of their excellent activity and selectivity. Among these options, Fe/ZSM-5 provides an optimal combination of catalytic activity and stability over a broad temperature range [24-26]. In the study, we prepared mesoporous ZSM-5 loaded by $FeCl_3$ by impregnation. The catalyst is applied to the purification process of lean-burn exhaust and its catalytic performance was studied. The purpose of this study is to replace expensive three way catalysts with non noble metal catalysts.

Experimental

Catalyst Preparation

Mesoporous ZSM-5 was prepared by alkali dissolving and desilication. Adding 3g original molecular sieve ZSM-5 (purchased from the Catalyst Plant of Nankai University, Si/Al=46, recorded as P) to 100mL 0.2mol/L NaOH solution, the solution was heated 2h by stirring 500rpm and refluxed at 65°C in a water bath. After the reaction is finished, cooling, filtering, washing, drying 10h at 110°C, the powder is obtained and weighed the powder, then calculated the mass loss of the molecular sieve. To obtain H-form, the obtained powder was exchanged 5h at 70°C in 0.5mol/L ammonium nitrate solution, then cooling, filtering, washing with deionized water, drying at 110 °C for 10h, repeated the ion exchange process three times. Finally, the treated ZSM-5 was calcined at 550 °C for 4h. The mesoporous ZSM-5 molecular sieve treated with 0.2mol/L NaOH solution was obtained and labeled as 0.2AT. According to the same operation method, the molecular sieve was treated with NaOH solution concentration of 0.3mol/L, 0.4mol/L, 0.5mol/L, 0.6mol/L, and the samples were labeled as 0.3AT, 0.4AT, 0.5AT, 0.6AT respectively.

The steps of using the impregnation method to prepare the ZSM-5 molecular sieve are as follows: a certain amount of ferric chloride was dissolved in ethanol, and then the 1g ZSM-5 molecular sieve was added to it, and all molecular sieves were just covered by the ethanol solution and stirred the solution for 1hr. ZSM-5 molecular sieve carrying ferric chloride was completely dried at 100°C. The catalyst was labeled as P-$FeCl_3$. The same method was used to prepare the mesoporous molecular sieves loaded with ferric chloride with NaOH concentration of 0.2-0.6mol/L, respectively, which were labeled as 0.2AT-$FeCl_3$, 0.3AT-$FeCl_3$, 0.4AT-$FeCl_3$, 0.5AT-$FeCl_3$, 0.6AT-$FeCl_3$, respectively.

Characterization

The BET surface area of the samples was determined using a volumetric adsorption apparatus (Micromeritics, Tristar3000) by N_2 adsorption at -196 °C. The specific surface area of the samples was calculated by the Brunauer -Emmett-Teller (BET) method, whereas the pore diameter was evaluated by applying the Barrett-Joyner-Halenda (BJH) algorithm to the isotherm desorption branch.

Powder X-ray diffraction (XRD) was performed with a Rigaku D/MAX2200 X-ray diffractometer by using Cu Kα (40 kV, 40 mA) radiation and a secondary beam graphite monochromator.

Sample morphology was studied by using a field emission scanning electron microscope (Hitachi S4800). Maximum acceleration voltage was set at 15 kV, and the sample was uniformly dispersed in the copper with a double-sided adhesive.

The surface acidity of the sample was determined by chemisorption instrument (Autochem2910 of Micromeritics, USA). 100mg of the sample is treated with 1h at 550 °C under He atmosphere. Cooling to room temperature, passed into the NH_3 until the adsorption saturation baseline is stable.

Then the He atmosphere is used to sweep 1h and clean the NH_3 on the surface of the sample. The program is heated to 600 °C at the ramping rate 10°C·min^{-1}.The NH_3 desorption signal was detected by TCD detector.

Catalytic Activity Measurements

The catalytic activity test was carried out using a flow reactor system by passing a stoichiometric reaction gas mixture containing CO ($\varphi(CO)=1000\times10^{-6}$), NO ($\varphi(NO)=500\times10^{-6}$), C_3H_6 ($\varphi(C_3H_6)=1000\times10^{-6}$) , O_2 ($\varphi(O_2)=4750\times10^{-6}$) and H_2O($\varphi(H_2O)$= 5%)diluted in N_2 at a rate of 100 cm^3 min^{-1} over 500 mg of catalyst (SV = 60,000 h^{-1}), which had been pretreated in situ in the flow of the reaction gas(10% O_2 and 90% N_2) at 120°C for 10 min. The activity was measured while raising the temperature from 120°C to 550 °C at a rate of 10 °C min^{-1}. Fourier Transform Infrared spectroscopy (MKS, MultiGas 2030 HS type) was used to detect the concentration of reactants and by-products at the outlet. The conversion rate of each reactant was calculated automatically.

Results and discussion

Catalyst characteristics

Fig. 1 shows the N_2 adsorption/desorption isotherms of the parent and the alkali treated zeolites at different alkali concentrations. Their physical characteristics are summarized in Table 1. The resulting BJH pore-size distribution curves were showed in Fig.2.

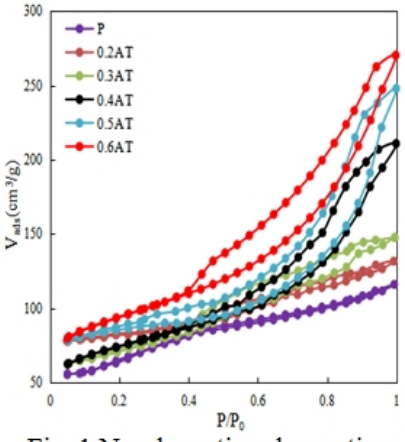

Fig. 1 N_2 adsorption desorption isotherms of the parent and the ZSM-5 treated with alkali solution

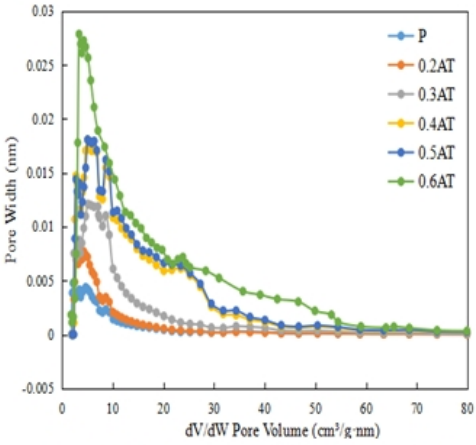

Fig. 2 BJH pore size distribution of the parent and the ZSM-5 treated with alkali solution

Table 1 Structural physical properties of ZSM-5zeolites treated by NaOH solution and zeolites loaded $FeCl_3$

Sample	W_{loss}[a] (wt.%)	S_{BET} (m^2/g)	S_{micro}[b] (m^2/g)	S_{meso}[c] (m^2/g)	V_{total}[d] (cm^3/g)	V_{micro}[b] (cm^3/g)	V_{meso}[c] (cm^3/g)	$D_{Pore\ Size}$ (nm)
P	-	235	158	77	0.171	0.085	0.086	4.8
0.2AT	15	299	203	96	0.194	0.090	0.104	6.5
0.3AT	34	311	174	137	0.236	0.122	0.114	7.2
0.4AT	46	322	169	153	0.345	0.047	0.298	8.2
0.5AT	60	348	160	188	0.374	0.065	0.310	8.3
0.6AT	62	346	154	192	0.408	0.082	0.326	8.5
P-$FeCl_3$	-	186	154	32	0.268	0.069	0.199	4.4
0.2AT-$FeCl_3$	-	243	147	96	0.274	0.058	0.216	6.0
0.3AT-$FeCl_3$	-	245	118	127	0.287	0.051	0.236	6.3
0.4AT-$FeCl_3$	-	195	112	183	0.327	0.044	0.283	6.7
0.5AT-$FeCl_3$		312	107	205	0.371	0.027	0.344	7.4
0.6AT-$FeCl_3$		293	86	207	0.382	0.025	0.357	7.4

[a]Weight loss；[b]t-plot Method； [d]N_2 volume adsorbed at p/p_0=0.99；

[c]$V_{meso}=V_{total}-V_{micro}$, $S_{meso}=S_{BET}-S_{micro}$.

From Fig.1, it is known that the parent molecular sieve (P) has a relatively flat adsorption and desorption isotherm, showing a typical I adsorption isotherm of the molecular sieve, indicating that the parent molecular sieve has a microporous structure without an appreciable contribution of mesoporosity (0.086 cm^3/g) which might be due to the presence of defects in the crystals and an intercrystalline porosity. When the ZSM-5 zeolite was treated with NaOH solution, the characterization results showed that the adsorption and desorption isotherms of all the samples showed an obvious hysteresis loop of IV type, indicating that the mesoporous structure had been produced by the treatment by the alkali solution. When the concentration of alkali solution is 0.2mol/L, the adsorption desorption curve is flat because of the low concentration of alkali concentration, and the mesoporous structure is not obvious when the concentration of alkali is low, but the adsorption / desorption curve of molecular sieve shows obvious mesoporous hysteresis due to the increasing of the concentration of alkaline solution. It can be seen that the total surface area and total pore volume of ZSM-5 zeolite after alkali treatment increased obviously from 235m^2/g and 0.171cm^3/g to 346m^2/g and 0.408cm^3/g respectively. At the same time, mesoporous surface area and mesoporous pore volume are also increased from 77m^2/g and 0.086cm^3/g to 192m^2/g and 0.326cm^3/g respectively. On the contrary, the micropore surface area and micropore volume showed a decreasing trend, but the decrease was small, from 158m^2/g, 0.085cm^3/g to 154m^2/g, 0.082cm^3/g, respectively, which indicates that the micropore system of the zeolite itself remains nearly unchanged. This indicates that the zeolite after alkali treatment still retains its microporous structure and produces mesoporous pores. At high alkali concentration, such as 0.5-0.6mol/L, due to serious desilication, ZSM-5 zeolite also has macropore structure.

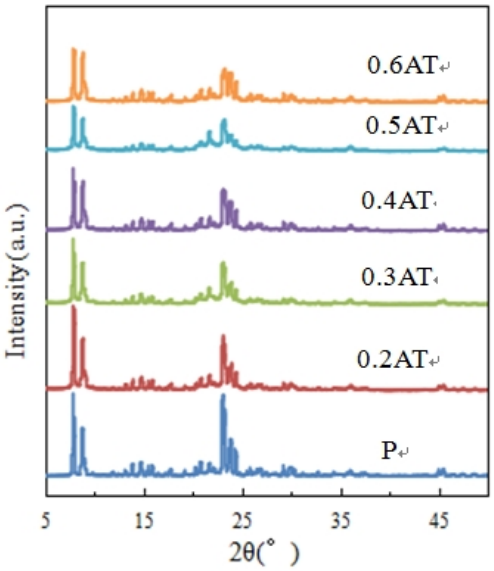

Fig. 3 XRD Diffraction Patterns of the parent and the ZSM-5 Treated with Different Alkali Concentrations

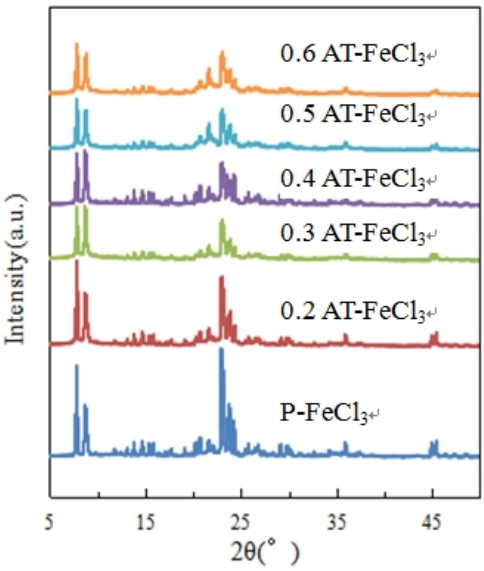

Fig. 4 XRD Diffraction Patterns of the zeolites loaded by $FeCl_3$

XRD Diffraction Patterns of the parent and the ZSM-5 treated with alkali solutions are shown in Fig.3. As can be seen, the main peaks of the ZSM-5 treated with alkali solutions are presented at the 2θ of 7-9°, 23-25°, respectively, which are in the range of typical specific peaks of ZSM-5. The sharp reflections also correspond to the MFI structure even after the strong alkaline treatment.

The crystallinity of the zeolite treated by alkali decreased gradually with the increase of alkali concentration. Through the study of the diffraction peak of the sample, it is found that the diffraction peak of the sample shifts to a high angle in the range of 2θ at 23-25°.It is deduced that the lattice spacing of molecular sieve shrinks due to alkali treatment, and the diffraction peak shifts

to a high angle. It is also possible that the silicon species, dissolved by the alkali, are loaded on the surface of the molecular sieve and then reentered into the lattice gap of the molecular sieve, which reduces the spacing of the crystal surface.

The XRD patterns of the $FeCl_3$/ZSM-5 samples are collected in Fig.4, which are similar to Fig 3. All zeolites have the MFI framework topology. In Fig. 4, no features belonging to large $FeCl_3$ particles were observed, which is indicative for the high $FeCl_3$ dispersion in the zeolites treated by alkali.

Fig. 5 is SEM images of the parent and the ZSM-5 treated with alkali solutions. The surface morphologies of the zeolites treated with different alkali concentrations can be clearly observed in Fig. 4. The parent molecular sieve P has a smooth surface a. However, it was observed after alkali treatment that the surface of the molecular sieve was uneven. When the alkali concentration is 0.2mol/L-0.3mol/L, because of the low concentration of alkali solution, there are only a few defects on the surface of the zeolite. With the increase of alkali concentration, the surface roughness of ZSM-5 zeolite is more obvious, and the surface of molecular sieve is shedding or even cracking. When the concentration of alkali reaches 0.6mol/L, the surface of the molecular sieve becomes very rough, the edge ruptures and is dissolved by alkali. The results are consistent with the results of XRD. The alkali solution acts on the molecular sieve to reduce the crystallinity of the molecular sieve.

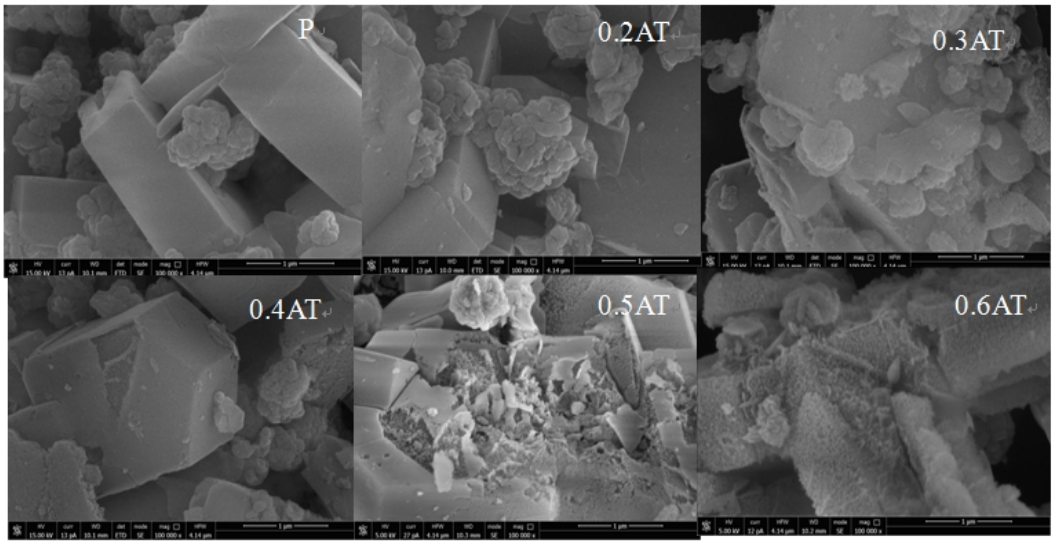

Fig. 5 SEM images of the parent and the ZSM-5 Treated with Different Alkali Concentrations

Fig. 6 is NH_3-TPD profiles of the parent and the ZSM-5 treated with alkali solutions. As can be seen from Fig. 6, the original molecular sieve has two typical NH_3 desorption peaks, of which the strong acid sites (Brønsted acid sites) desorption peak is at the higher temperature (350~550°C), and the lower temperature (100~350 °C) is the weak acid sites (L)

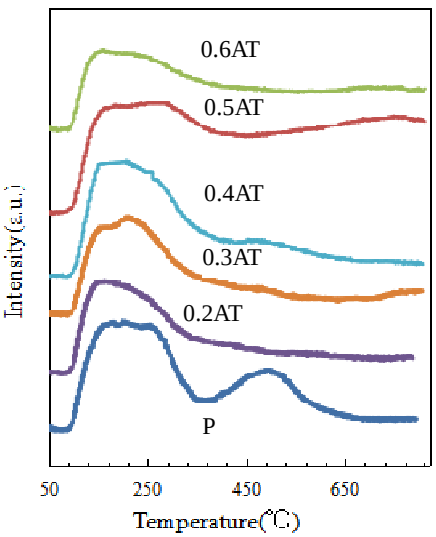

Fig.6 NH_3-TPD profiles of the parent and the ZSM-5 Treated with Different Alkali Concentrations

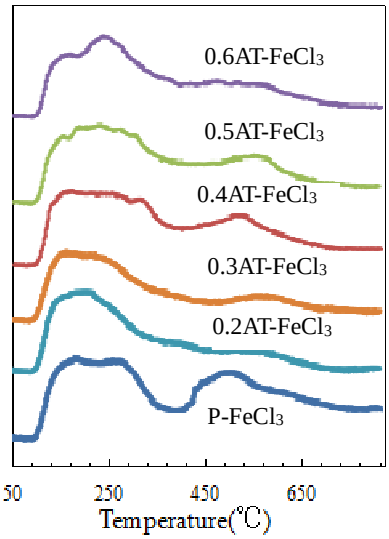

Fig. 7 NH_3-TPD profiles of ZSM-5 Supported $FeCl_3$

desorption peak. With the increase of concentration of alkali solutions from 0.2 mol/L to 0.6mol/L, the desorption peak of strong acid sites weakens, while the NH_3 desorption peaks of weak acid sites increase. This is due to the desilication of alkali treatment, resulting in the formation of more Al Lewis acid sites. Brønsted acid peak intensity gradually weakened, this may be the breakdown of Si-OH-Al bridge and the ion exchange of Na^+ instead of H^+ during the alkali treatment process. When $FeCl_3$ loaded on ZSM-5, $FeCl_3$-ZSM-5 samples are shown in Figure 7. NH_3 desorption peaks of weak acid sites increase and a new strong acid sites (Brønsted acid sites) desorption peak appears at the higher temperature (500~ 600°C). Especially, when ZSM-5 treated by concentration of alkali solutions was 0.5 mol/L.

Exhausting gas cleaning performance of Fe-ZSM-5

The concentration curves of reactant with the change of temperatures by ZSM-5(0.5) and Fe-ZSM-5(0.5) were shown in Fig.8 and Fig.9, respectively. The mesoporous molecular sieve ZSM-5 (0.5) and the mesoporous molecular sieve Fe-ZSM-5 (0.5) loaded with $FeCl_3$ are used as catalysts to treat the simulated automobile exhaust CO, NO and C_3H_6. As the reaction temperature increases, the concentration of CO, NO and C_3H_6 gradually decreases. When ZSM-5 (0.5) is used as catalyst, the concentration tends to be constant the temperature is 430°C. While Fe-ZSM-5 (0.5) is used as catalyst, when the temperature is 400, the concentration tends to be constant and the conversion of C_3H_6 reaches 100%, which indicates that the catalytic effect of mesoporous molecular sieve loaded with $FeCl_3$ is more active.

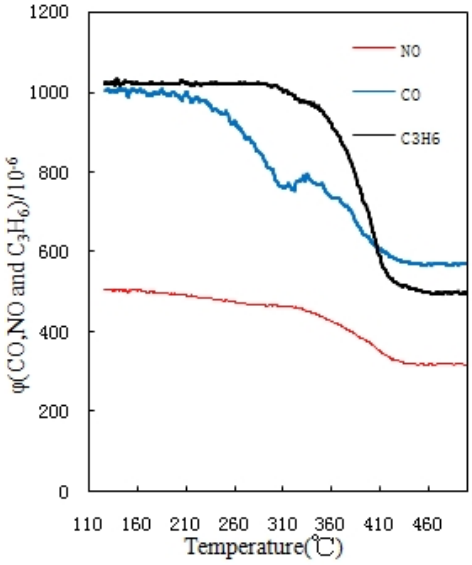

Fig.8 The concentration curves of reactant with the change of temperatures by ZSM-5(0.5)

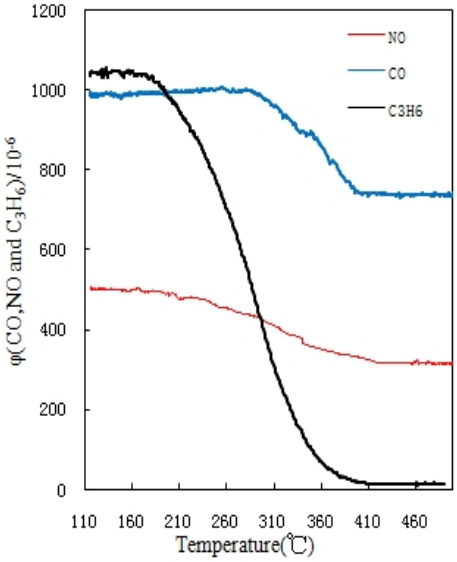

Fig. 9 The concentration curves of reactant with the change of temperatures by Fe-ZSM-5(0.5)

Conclusions

Mesoporous ZSM-5 zeolites can be obtained by alkali treatment ZSM-5 zeolites. The mesoporous surface area and mesoporous pore volume after alkali treatment increased obviously increasing alkali concentration to 0.5M. The crystallinity of the zeolite treated by alkali decreased gradually with the increase of alkali concentration. The XRD patterns of the $FeCl_3$/ZSM-5 samples show that the high $FeCl_3$ dispersion in the zeolites treated by alkali. All zeolites have the MFI framework topology. When Fe-ZSM-5 is used as catalyst for Cleaning auto-exhaust, the catalytic effect of mesoporous molecular sieve loaded with $FeCl_3$ is more active than HZSM-5.

Acknowledgements

This work was financially supported by the National Natural Science Foundation of China (31060099, 3070062).

References

[1]R.M. Heck, R.J. Farrauto, Applied Catalysis A: General, Vol. 221. (2001), p. 443-457.
[2] J. Kaspar, P. Fornasiero, N. Hickey, Catalysis Today, Vol. 77. (2003), 419-449.
[3] M. Konsolakis, LV. Yentekakis, Topics in Catalysis, 56. (2013), 165-171.
[4] A. Konig, G. Herding, B. Hupfeld, T. Richter, K. Weidmann, Topics in Catalysis, Vol.16.(2001), 23-31.
[5] M.V. Twigg, Applied Catalysis B: Environmental, Vol. 70, (2007), 2-15.
[6] M. Machida, S. Minami, S. Hinokuma, H. Yoshida, Y. Nagao, T. Sato, Y. Nakahara, The Journal of Physical Chemistry C, Vol.119. (2015), 373-380.
[7] J. Wang, H. Chen, Z. Hu, M. Yao, Y. Li, Catalysis Reviews: Science and Engineering, Vol.57. (2015), 79-144.
[8] Q. Wang, G. Li, B. Zhao, R. Zhou, Journal of Hazardous Materials, Vol.189 (2011), 150-157.
[9] R.W. McCabe, R.K. Usmen, Studies in Surface Science and Catalysis, Vol.101. (1996), 355-368.
[10] Y. Nagao, Y. Nakahara, T. Sato, H. Iwakura, S. Takeshita, S. Minami, H. Yoshida,M. Machida, ACS Catalysis, Vol.5.(2015), 1986-1994.
[11] S.B. Kang, I. Nam, B.K. Cho, C.H. Kim, S.H. Oh, Chemical Engineering Journal, Vol. 259. (2015), 519-533.
[12] M.P. González-Marcos, B. Pereda-Ayo, A. Aranzabal, J.A. González-Marcos, J.R González-Velasco, Catalysis Today, Vol.180. (2012), 88-95.
[13] P.S. Lambrou, A.M. Efstathiou, Journal of Catalysis, Vol.240. (2006), 182-193.
[14] R.A. Daley, S.Y. Christou, A.M. Efstathiou, J.A. Anderson, Applied Catalysis B: Environmental, Vol. 60. (2005), 117-127.
[15] K. Rahkamaa-Tolonen, T. Maunula, M. Lomma, M. Huuhtanen, R.L. Keiski, Catal. Today. Vol.100 (2005) ,217-222.
[16] M. Koebel, M. Elsener, M. Kleemann, Catal. Today. Vol. 59 (2000), 335-345.
[17] J.A. Sullivan, J.A. Doherty, Appl. Catal. B. Vol.55 (2005), 185-194.
[18] P. Forzatti, Catal. Today. Vol.62 (2000), 51-65.
[19] R.Q. Long, R.T. Yang, J. Catal. Vol.188 (1999), 332-339.
[20] D. Berthomieu, N. Jardillier, G. Delahay, B. Coq, A. Goursot, Catal. Today. Vol.110 (2005), 294-302.
[21] O. Krocher, M. Devadas, M. Elsener, A. Wokaun, N. Soger, M. Pfeifer, Y. Demel, L.Mussmann, Appl. Catal. B. Vol.66 (2006), 208-216.
[22] A.A. Battiston, J.H. Bitter, F.M.F. de Groot, A.R. Overweg, O. Stephan, J.A. van Bokhoven, P.J. Kooyman, C. van der Spek, G. Vanko, D.C. Koningsberger, J. Catal. Vol.213. (2003), 251-271.
[23] M.S. Kumar, *On the Nature of Different Fe Sites in Fe-Containing Micro and Mesoporous Materials and Their Catalytic Role in the Abatement of Nitrogen Oxides from Exhaust Gases*, Disseration, Humbold-Universitat, Berlin, 2005.
[24] G.D. Pirngruber, P.K. Roy, R. Prins, Phys. Chem. Chem. Phys. Vol.8. (2006), 3939-3950.
[25] S. Brandenberger, O. Krocher, A. Tissler, R. Althoff, Catal. Rev. Sci. Eng. Vol.50. (2008),492-531.
[26] S. Brandenberger, O. Krocher, A. Tissler, R. Althoff, Appl. Catal. A: Genet. Vol. 373. (2010), 168-175.